LIPS N.V. - DRUNEN - NEDERLAND

On the actuating forces of controllable pitch propellers.

Blade control by ventilation

Paper to be presented at the exhibition "Inrybprom", Leningrad, U.S.S.R., 19. August 1968

By: Ir. L.A. van Gunsteren

On the actuating forces of controllable pitch propellers

Blade control by ventilation

Summary

The costs and the engineering problems of the mechanism of any controllable pitch propeller are strongly dependent on the magnitude of the blade spindle torque. The blade spindle torque can be split into three parts: a. hydrodynamic torque, a friction torque and an inertia torque due to the centrifugal force.

The paper discusses the possibility of minimizing the hydrodynamic blade spindle torque by means of ventilation through holes on the face of the blade. The influence of the ventilation on the blade spindle torque is analysed by means of extended computer calculations.

The two dimensional pressure distribution of the ventilated sections is calculated with a linearized theory for lifting foils at zero cavitation number (9). Blockage and interference effects in the ventilated condition are neglected.

The distortion of the mean lines due to pitch setting is taken into account. The induced velocities by the free vortex system are calculated with a special lifting line theory, which has been adapted to heavy loadings by means of some empirical factors.

As an example an existing c.p.p. of a trawler is analysed. It is concluded that ventilation is a promising tool for the realization of c.p.p. designs with low blade spindle torque.

Introduction.

Controllable pitch propellers (c.p.p.) are increasing in number and size at an amazing rate.
We may expect this tendency to continue also in the future, as automation in ships becomes more and more common practice.
It is therefore deemed useful to ponder the conception of c.p.p. design in its present stage.

Obviously the engineering effort and the costs needed for the realisation of a c.p.p. installation are directly dependent on the magnitude of the actuating forces. These are the forces to be produced by the actuating mechanism for the changing of pitch during operation.
The actuating forces are proportional to the blade spindle torque, that is the torque with respect to the spindle axis required to change pitch.

In modern large c.p.p. installations, with over 25.000 horse power which is not exceptional any more, the blade spindle torque can bring the actuating force (e.g. in the actuating rod) easily over 200 tons. The immense engineering problems of such heavy loadings put a serious limit on the realisation of the shipowners wishes concerning the c.p.p. A drastic decrease of the blade spindle torque, without affecting other aspects, could therefore mean an important step forward.
How can this be achieved?

The blade spindle torque is made up of three parts (see (1)):

- a torque due to hydrodynamic forces
- a torque due to mechanical friction
- an inertia torque due to centrifugal forces.

The inertia torque is much smaller than the hydrodynamic and the friction one, although it should be taken into account in quantative calculations of blade spindle torque.
The friction torque depends directly on the hydrodynamic torque which itself is roughly half the total blade spindle torque. Significant gains are thus only to be expected from a reduction in the hydrodynamic blade spindle torque.

Of course many attempts have been made to reduce the hydrodynamic spindle torque, for instance by choosing:

- a pitch distribution which decrease strongly towards the blade root (flat blades).
- suitable blade sections
- a suitable rake
- a suitable skew (or blade outline and location of spindle axis)

Of these means only the application of skew back has no significant additional disadvantages. Flat blades spoil the efficiency seriously in the order of 15%, and rake increases the stresses in the blades and hub construction due to centrifugal forces, resulting in additional weight. The selection of two dimensional sections is determined by cavitation requirements.

It is not possible, however, to choose the skew in such a way, that a low hydrodynamic spindle torque is obtained over the whole range of operation. A useful improvement is therefore only to be expected from hydrodynamic means, which can be temporarily used and do not affect the performance of the propeller in the design condition.
Such a solution may be found in movable flaps, which involves, however, serious mechanical problems.
A more practical means for the control of the pressure distribution over the blades may be the injection of air (or other gasses) through holes in the blades, the air being supplied through tubes in the shaft and actuating mechanism.
It is the aim of this paper to investigate and discuss this idea.

Nature of the blade spindle torque.

Let us have a look at an ordinary right handed c.p.p.
In the design condition the entrance will be nearly shock free - that means the stagnation point is located on the nose of the profile - and consequently the pressure distribution over the chord of a blade element will have an elliptic character. The resulting lift force of this pressure distribution acts about mid-chord or slightly forward of it, as for instance when the N.A.C.A. a = 0.8 mean line is used.
It is logical to select the skew in such a way that the maximum spindle torque encountered in the whole range of operation is minimized.

This requirement generally yields a moderate and negative hydrodynamic spindle torque in the design condition (outwardly directed torque vectors are defined to be positive).
Thus, the hydrodynamic loading "tries" to put the blade in the astern position.
In this way the point where the spindle torque changes direction and flutter might occur, is kept outside (above) the range of operation.

Decreasing the pitch, so that the effective angle of attack tends to become negative, we obtain a pressure distribution which can be thought to be made up of three parts:

- a basic pressure distribution associated with the camber of the section, this is the design pressure distribution.
- a pressure distribution of a non cambered profile(flat plate) under a negative angle of attack.
- a pressure distribution associated with the distortion of the mean line due to pitch changing.

These three pressure distributions are schematically indicated in figure 1.

The nature of the distortion of the mean line due to the decrease in pitch requires explanation. Figure 2 gives the axial projection of the outline of a propeller blade, looking from aft in the sailing direction.

Consider the mean line of the section C-T-A on radius X_A. For sake of simplicity we assume this mean line to be flat in the design condition.
By a pitch decrease of an angle $\Delta\alpha$, the section mean line on radius X_A becomes D_1-T-B_1.
The points B_1 and D_1 originate from the points B and D. As these points are situated more inward than the points A and C, their local pitch angles have to be larger. Consequently, the local pitch angles at the points B_1 and D_1, are also larger than those of the points A and C.
The resulting mean line is not flat any more, but has a S-shaped form as indicated in figure 3. A second consequence of this effect is, that the nose - tail line has turned over a smaller angle than the blade itself, as will be clear from figure 3.
Especially at large pitch deviations, both the additional pitch angle of the nose - tail line and the distortion of the mean line have a considerable influence on the pressure distribution. We developed an interative procedure, which can calculate the shape of the distorted mean line of a section at a given pitch angle deviation from the design position. This procedure has been incorporated in all our computer programs concerning the hydrodynamics of controllable pitch propellers.

It will be clear from figure 1, that both the "flat plate" pressure distribution and the "distortion" pressure distribution have an increasing effect on the blade spindle torque. Consequently we may expect the hydrodynamic blade spindle torque to increase the more the angle of attack becomes negative and the more the pitch is put astern.
In practice, however, the largest actuating forces are not met in the astern condition, but in the vicinity of the point of zero thrust. This is caused by the effect of cavitation which considerably affects the pressure distribution at negative pitch settings. In particular the "flat plate" pressure distribution is "cut off" by the cavitation number.

As in the partially cavitating condition the lift is known to be hardly effected, the cut off "pressure area" at the nose will be compensated by an approximately equal additional area at the rear of the chord. The larger the region of cavitation, the more favourable the pressure distribution will be with regard to the blade spindle torque.

The characteristic curve of the blade spindle torque as a function of the pitch settings at constant rotational speed of the propeller is indicated in figure 4.
Non cavitating sections at negative pitch setting can be met in practice when the blade area is exeptionally large. In such cases the maximum blade spindle torque occurs at maximum negative pitch, as is indicated with a dot-dash line in figure 4.
The favourable effect of cavitation upon the magnitude of the hydrodynamic blade spindle torque already suggests that an important gain may be achieved by enlarging this influence artificially by means of ventilation.
The friction blade spindle torque is always directed against the movement itself. Thus, the largest (negative) spindle torques occur putting the pitch from astern to ahead. The total spindle moment is indicated by a thick line in figure 4. The friction spindle torque depends on all six force and torque components exerted by the blade onto the hub; it may behave discontinuously if one of these components changes sign and the origin of the friction is abruptly changed from one surface in the mechanism to another.

We have indicated in figure 4 five characteristic points:

1. Point of zero thrust
2. Bollard condition ahead
3. Bollard condition astern
4. Free running ahead
5. Free running astern.

Although more severe situations with regard to blade spindle torque are imaginable - e.g. the manoeuvre from ahead to astern and immediately again to ahead -, we feel that these five conditions determine sufficiently the actual situation. For many cases the picture is even on the pessimistic side, because mostly there is no need to run through the zero pitch point at maximum rotational speed of the propeller. Already a small reduction in r.p.m. at this point considerably lowers the blade spindle torque.
In our analysis of the merits of ventilation with respect to the actuating forces, we shall calculate these forces for the five conditions defined above in both the non ventilated and the ventilated condition.

Calculation of actuating forces in non ventilated condition

Figure 5 shows a simple flow chart of the calculation of the actuating forces in one of the five characteristic operating conditions.
As it is beyond the scope of this paper to present a detailed description of the applied theories and methods, only the essence of them will be given.

The distortion of the mean lines (box 2 of figure 5), as described above, is calculated assuming that the section is flat in the design condition. The resulting S-shaped mean line is simply added to the design mean line and the turning of the nose-tail line is incorporated in the pitch angle.

The calculation of the two dimensional section characteristics (box 3 and box 5 of figure 5) is done by the method described in section 4.5 of reference (2). In this method the velocity distribution about the wing section is considered to be composed of three separate and independent components:

- the distribution corresponding to the velocity distribution over the basic thickness form at zero angle of attack.
- the distribution corresponding to the load distribution of the mean line at its ideal angle of attack.
- the distribution corresponding to the additional load distribution associated with angle of attack.

These three basic velocity distributions have been tabulated in reference (2) for families of thickness forms and mean lines, the tables being computed by conformal mapping techniques. When proper corrections for viscosity are applied, the pressure coefficients obtained by this method are considered to be very accurate.
In order to be able to use the tables of reference (2), any mean line is thought to be made up of several tabulated meanline types.

The effect of cavitation is taken into account as follows. If the under pressure coefficient at any point of the suction side would exceed the cavitation number, the area cut off by the cavitation number at the entrance is distributed over the rear of the chord. This additional pressure distribution is assumed to decrease linearly over the rear of the chord towards zero at the trailing edge.

The iterative lifting line procedure (box 4 of figure 5) is similar to the method described in reference (3); it differs, however, basically in the application of correction factors. Basic assumption is, that the sections can be calculated independently. This is in fact only correct for propellers with an optimum radial load distribution. We got round this difficulty by introducing proper correction factors. Starting point is the well known equation of optimum lifting line propellers (see reference (4) section 41):

$$C_L = \frac{4\pi D}{Z\,C} \cdot x \cdot \kappa \cdot \sin\beta_i \cdot \tan(\beta_i - \beta) \qquad (1)$$

where:

C_L = lift coefficient of the section
D = propeller diameter
x = dimensionless radius
Z = number of blades
C = chord length
β = pitch angle of undisturbed inflow direction.
β_i = pitch angle of inflow direction corrected for velocities induced by the free vortex system.

K = Goldstein factor, allowing for the effect of finite number of blades.

Usually an additional correction - for instance that of Ludwieg und Ginzel - on camber is applied, allowing for stream curvature (lifting line-lifting surface correction).
In our method neither Goldstein, nor Ludwieg und Ginzel corrections are applied. Instead a correction on the induced velocity is used, which includes:

- effect of number of blades
- effect of aspect ratio (lifting line-lifting surface correction)
- effect of propeller load (slip stream contraction)

The correction has been found by an extended regression analysis of systematic propeller series. Bringing the lift gradient to the right side of equation (1), we can write it in form:

$$\alpha = f(\alpha) \qquad (1a)$$

where:

α = angle of attack measured from zero lift direction.
This equation can conveniently be solved by Wegstein's iterative method (see reference (4)).

It seems useful to give an impression of the accuracy of the methods described so far. Figure 6 gives the particulars of a controllable pitch propeller of a trawler. We will use this propeller as an example throughout this paper. Figure 7 presents the open water diagram of this propeller calculated with the methods described above.
Also the characteristics of a comparable Troost propeller have been drawn. Not only from the agreement showed in figure 7, but also from experience with this method in many other cases, it may be concluded that it possesses sufficient accuracy.

Once the pressure distribution is determined, the hydrodynamic forces and torques are obtained by chordwise and radial integration (box 8 of figure 5). As an example of the expressions involved, we present in appendix 1 the formula for the hydrodynamic torque component with respect to the spindle axis. Expressions for the other five hydrodynamic force torque coefficients are found in a similar way.
The numerical integration of the centrifugal forces involves no particular difficulties (box 9 of figure 5).

Once the forces exerted by the blade onto the hub are determined, the consequent friction forces in the mechanism are calculated and added (box 10 of figure 5). Of course, the choice of friction coefficients involves some uncertainty.
This completes the calculation of the actuating forces.

In order to give an impression of the accuracy of the procedure described above, the results of calculations for the propeller of figure 6, as well as full scale measurements of it are presented in figure 8.
In view of the many approximations involved, we feel that the agreement is sufficient, in any case for the present analysis.

The ventilated condition.

It will be obvious, from the considerations of the second section and our example presented in the preceeding section, that the severest condition is putting the pitch from astern to ahead, at about zero - or in some cases at negative - pitch settings. The most significant contribution to the negative hydrodynamic blade spindle torque can be expected to originate from the "flat plate" pressure distribution at negative angle of attack. See figure 1. We can reduce the strength of this distribution by ventilating air through the face of the blade, that is the nominal pressure side, now acting as a suction side. We assume air inlets to be located on the face at 5% from the leading edge. The air pressure is assumed to be equal to the free stream pressure; that means that the cavitation number based on cavity pressure is zero and the cavity, starting from the nose of the section, is infinite in extent. It is known from the theory of fully cavitating foils. This means that the reduction in the effect of the flat plate pressure distribution of figure 1 may be expected to be of the same order. Hence that the lift gradient is only one quarter of that of the subcavitating foil.

Based on the finding of reference (6), in which the requirements for ventilation inception are investigated, we may expect that this point will not present any difficulties in practice. A very favourable circumstance in this respect is that in the considered condition the angle of attack and the camber have opposite sign, yielding a pronounced under pressure peak at the leading edge. In our calculations we shall assume arbitrarily the ventilation to start, if in the non ventilated condition the under pressure coefficient at the 5% chord point exceeds 0.05.

Another point of practical importance consists of the air requirements, because these will determine the air supply measures such as the tubes in the blades and actuating mechanism.
This problem has been investigated in reference (7).
In view of the results of this reference, we may state that also this point will not present serious problems. In order to get an impression of the feasibility of the air supply system, we made several designs of the hub mechanism with such systems built in.

The idea of ventilation being feasable at a first glance, we now have to make quantitative calculations of the reduction in blade spindle torque. This is not so easy, because a three dimensional theory for the analysis of fully cavitating propellers is not yet available. We therefore shall proceed as follows.
In the computer program the described test on ventilation inception is built in. If ventilation occurs, all two dimensional calculations of the considered section are replaced by procedures for the analysis of ventilated lifting foils in two dimensional flow.
This concerns box 3. and 5 of figure 5.
Earlier design methods of supercavitating propellers were based on this principle, which has led, however, to over - optimistic predictions.
The discrepancy can be explained by two important effects, namely cavity blockage and cavity - blade interference. See reference (8).
These effects influence the lift of the blade sections. But it is not to be expected that they will have a strong effect on the distribution of

pressure along the chord, this being the key point of the present study. In view of this we shall neglect cavity blockage and blade interference in our calculations.
We assume that the sections are only ventilated during pitch changing. Consequently the pitch positions of the five characteristic operating conditions are identical in both the ventilated and the non ventilated condition. Calculating with the corresponding pitch settings of the non ventilated condition, we may therefore omit for the ventilated case the iteration on horse power (box 6 of figure 5).
Also the procedures concerning partially cavitating conditions are skipped, because these regions are ventilated now.
The pressure distributions in two dimensional ventilated flow are calculated with the linearized theory for fully cavitating foils at zero cavitation number of Tulin and Burkart (9). In this theory the fully cavitating hydrofoil is reduced to an equivalent aitofoil, which can be analysed by classic thin airfoil theory.
The results of reference (9) used in our study are reviewed in appendix 2.
We analysed the equivalent airfoil by Glauert's method, taking 30 sinus-coefficients in the Fourier expansion throughout all calculations.
Test calculations for a flapped hydrofoil, which is obviously not very suited to Fourier analysis, yielded pressure distributions agreeing within a few percent with the measurements of Meijer (10).

We have to deal with the case of a fully cavitating foil with negative camber and positive angle of attack. See figure 9.
This has some consequences. Analising this configuration we arrive at under pressures at the wetted side. In naturally fully cavitating flow this would be a physically impossible solution, because cavitation would occur at such points. In artificially cavitating flow such solutions are acceptable, provided, of course, that the under pressure coefficient does not exceed the cavitation number based on vapor pressure.
The drag characteristics of such negative cambered fully cavitating foils are very poor. We found indeed in our calculations that by ventilating the blades, the drag coefficients of the sections will increase considerably. This may be a useful circumstance. In the ventilated condition the lift is strongly reduced, so also the torque on the propeller shaft will decrease considerably. This may be unfavourable with regard to the characteristics of the machinery.
The fact that fully cavitating foils are so much more sensible to profile form than subcavitating foils, works also in an unfavourable sense.
Test calculations showed that the negative moment coefficient of negatively cambered sections is in fully wetted flow only about 2/3 of that in fully cavitating flow. This works out unfavourably with respect to the blade spindle torque. The effect is stil enlarged by the fact that the negative camber of the wetted side of the fully cavitating section is half the blade thickness larger than the camber of the mean line of that section. Also the effect of the S-shaped form of the section due to the distortion is increased in the ventilated condition.
In view of these considerations, we also included the possibility of ventilation on two sides of the blade.
We proceeded as follows. If the considered section is already ventilated on the face, the pressure coefficient at 70% of the chord from the entrance is tested. If the under pressure coefficient exceeds 0.05, it is assumed that the back of the section is also ventilated. The free stream line is assumed to spring off from the 70% chord point, so that the rear of the section is over 30% of the chordlength entirely within the cavity.

In order to establish this situation extra air inlets have to be provided on the back of the blade slightly behind the 70% chord point. It should be noted that the conditions for cavitation inception are less favourable than at the inlets on the face of the blade.
How serious this problem is, can only be explored by means of experiments.

Results.

Having available the tools for the calculation of the actuating forces both in non ventilated and in ventilated conditions, we are now able to present the results of the analysis of our example. The propeller is defined in figure 6, the radial wake distribution and the mean inflow velocities for the free running conditions are given in table 1.

The force in the actuating rod as a function of the pitch angle at maximum rotational speed is presented in figure 10.
Four dimensionless constants K_Q, K_T, CRH, CRHI, defining the shaft torque, the thrust, the hydrodynamic blade spindle torque, the frictionless blade spindle torque (i.e. hydrodynamic plus intertia torque) respectively, are given in table 2 for the five characteristic operating conditions in ventilated and non ventilated cases. In particular the torque constant K_Q deserves attention, because it affects the working of the main engine.
The corresponding pressure distributions at .7 radius are presented in figure 11 up to and including 14. At positive pitch settings we find of course approximately the design pressure distribution, being in our example that of the N.A.C.A. $a=.8$ mean line.

The result indicate a significant reduction in the magnitude of the actuating force at negative pitch settings in the ventilated conditions over the non ventilated ones.
As could be expected, the most advantage is obtained when we ventilate at two sides. If we ventilate only the face of the blade the reduction in blade spindle torque is also considerable. This suggests that in the first place further research could be limited to ventilation at one side.

As can be seen from figure 10 the largest forces in the ventilated conditions are not met at small pitch angles any more, but at positive pitch settings (bollard and free running ahead). The blade spindle torque at positive pitch settings can be lowered by decreasing the design skew. Calculating with half the original skew, we get the results presented in figure 15 up to and including 19 and table 3.
As one sided ventilation seemed the most feasible, we limited the calculation to that case. It can be seen from figure 15 that the zero thrust point again shows the largest spindle torque within the range of operation. This critical value is less than one half of the corresponding maximum torque in the non ventilated condition (figure 10).

Conclusion.

The following conclusions can be made from our investigation.
The calculation of actuating forces of controllable pitch propellers with a digital computer seems to be sufficiently accurate, provided

that proper allowances are made for:

- the effect of heavy loading in the three dimensional analysis.
- the distortion of mean lines due to pitch changing.
- the effect of cavitation on the chord-wise pressure distribution.

Ventilation through holes on the face of the blade can lower the actuating forces by more than 50%. This seems therefore to be worth further research. In order to check the promising results of this paper, model tests should be carried out, including the aspects of ventilation inception, air requirements and optimum location of air inlets.

Acknowledgement.

The inspiring support of Prof. Dr. Ir. J.D. van Manen, Director of the Netherlands Ship Model Basin at Wageningen is gratefully acknowledged. The author is indebted to his co-worker Mr. W.A. Arnoldus, Head of the Computer Department of Lips N.V., who developed the procedures concerning the subcavitating range. Appreciation is expressed to Mr. M.M.H. Lips, President Director of Lips N.V., for giving his permission to publish the results. The Nederland-U.S.S.R.-Instituut is thanked for the translation of the paper into Russian.

References.

(1) H. Klaassen and W. Arnoldus: "Actuating forces in controllable pitch propellers", Transactions of the Institute of Marine Engineers, Vol. 76, June 1964. 1048 D

(2) I.H. Abbott and A.E. von Doenhoff: "Theory of wing sections", Dover Publications, Inc., New York, 1959.

(3) J.E. Kerwin: "Machine computation of marine propeller characteristics", International Shipbuilding Progress, Vol. 6, no. 60, August 1959.

(4) G.N. Lance: "Numerical methods for high speed computers", Iliffe, London, 1960, pp. 134-138.

(5) J.D. van Manen: "Fundamentals of Ship resistance and propulsion". Part B: Propulsion. Publication no. 132 a of the N.S.M.B., International Shipbuilding Progress 1960.

(6) R.A. Barr: "Ventilation inception", Hydronautics, Inc., Technical Report 127'4, March 1963.

(7) R.A. Barr: "Air requirements for ventilated propellers", Hydronautics, Inc., Technical Report 127-5, March 1963.

(8) M.P. Tulin: "Supercavitating Propellers, History, Operating Characteristics and Mechanism of Operation", Proceedings of the Fourth ONR symposium on Naval Hydrodynamics (Government Printing Office), Washington, D.C. 1962.

(9) M.P. Tulin and M.P. Burkart: "Linearized theory for flows about lifting foils at zero cavitation number", David Taylor Model Basin, Report C-638, February 1955.

(10) M.C. Meijer: "Pressure measurement on flapped hydrofoils in cavity flows and wake flows", Journal of Ship Research, vol. 11, no. 3, September 1967. 1359 F

Appendix 1

Formula for the hydrodynamic blade spindle torque.

Any point P is located on a chordwise distance a.c forward of mid-chord, the spindle axis intersection point T on a distance b.c. The pitch angle of the section is $\varphi(x)$. Then the projection on the propeller plane of the angle between the radius O-P and the radius O-T is:

$$\psi(a,x) = \frac{2.(a-b(x)).c(x).\cos\varphi(x)}{x\ D} \qquad (2)$$

where: $c(x)$ = chord length
x = dimensionless radius
D = propeller diameter

The free stream velocity, corrected for velocities induced by free vortexes, is V(x), its direction is determined by a pitch angle $\beta_i(x)$. The rotational speed is n; the fluid density is ρ.
The local pressure coefficient is PR(a,x), the local resistance coefficient is CD(a,x). We then can write for the dimensionless hydrodynamic blade spindle torque:

$$CRH = \frac{\text{hydrodynamic blade spindle torque}}{\rho D^5 n^2}$$

$$= .25 \int_{x=x_{hub}}^{1.} \left(\frac{V(x)}{n D}\right)^2 \frac{c(x)}{D} \int_{a=-.5}^{.5} \Big\{ \Big(PR(a,x).\cos\beta_i(x) - CD(a,x). \sin\beta_i(x) \Big) \frac{x}{2} . \sin\psi(a,x) + \Big(PR(a,x)\sin\beta_i(x) + CD(a,x)\cos\beta_i(x) \Big) \cos\psi(a,x) \frac{c(x)}{D} (a-b(x)).\sin\varphi(x) \Big\} da\,dx$$

(3)

Appendix 2

Results of linearized theory for flows about lifting foils at zero cavitation number.

The authors of reference (9) have been able to prove that the problem of a fully cavitating hydrofoil at zero cavitation number ($\sigma = 0$) is in its linearized version equivalent to an airfoil problem ($\sigma = \infty$), whose well known solution can easily be converted into the solution of the hydrofoil problem.

Maintaining the symbole of reference (9), we define:

Origin of system of coordinates x-y at the nose of the foil

x axis in undisturbed flow direction

y axis upwards

u,v = x and y components of perturbation velocity

U_∞ = uniform velocity at infinity, parallel to the x axis

Subscript o indicates quantities determined on the body surface.

Unbarred symbols refer to cavity flow.
Barred symbols refer to the non cavity flow.

It then can be proved by conformal mapping technique, for which we refer to (9), that the airfoil equivalent to any given hydrofoil is such that:

$$v(x) = \bar{v}(\sqrt{x})$$
$$u(x) = \bar{u}(\sqrt{x}) \qquad \text{or} \quad \frac{dy_o}{dx}(x) = \frac{d\bar{y}_o}{d\bar{x}}(\sqrt{x}) \tag{4}$$

and
$$\bar{U}_\infty = U_\infty \tag{5}$$

From these expressions we obtain the relation between the pressure coefficients PR and $\overline{PR}$:

$$PR(x) = \frac{1}{2}\,\overline{PR}(\sqrt{x}) \tag{6}$$

The identity (4) defines the equivalent airfoil, whose pressure distribution is calculated by classical thin airfoil theory.
This pressure distribution is converted into the pressure distribution of the hydrofoil by means of (5) and (6).

The airfoil pressure distribution can be found by Glauert's method, which gives the following.
The linearized boundary condition yields:

$$\bar{v}(\bar{x},0) = \bar{U}_\infty \frac{d\bar{y}_o}{d\bar{x}}(\bar{x}) = \frac{1}{\pi}\int_0^c \frac{\bar{u}(\bar{x}',0+)}{\bar{x}'-\bar{x}}\,d\bar{x}' \tag{7}$$

where $\bar{u}(\bar{x},0+)$ can be imagined as a vortex distribution replacing the actual airofoil.
It is assumed that the pressure distribution can be expanded in the series:

$$\bar{u}(\bar{x},0+) = \frac{1}{4}\,\overline{PR}(\bar{x})\,\bar{U}_\infty = \bar{U}_\infty\left(A_0 \cot\frac{\vartheta}{2} + \sum_{n=1}^{\infty} A_n \sin n\vartheta\right); \quad \bar{x}/c = \tfrac{1}{2}(1-\cos\vartheta) \tag{7a}$$

Then the relation between the airfoil shape and the Fourier coefficients follows from (7):

$$\frac{d\bar{y}_o}{d\bar{x}}(\vartheta) = -A_o + \sum_{n=1}^{\infty} A_n \cos n\vartheta \qquad (8)$$

where:

$$A_o = -\frac{1}{\pi}\int_0^{\pi} \frac{d\bar{y}_o}{d\bar{x}}(\vartheta)\, d\vartheta$$

$$A_n = \frac{2}{\pi}\int_0^{\pi} \frac{d\bar{y}_o}{d\bar{x}}(\vartheta) \cos n\vartheta\, d\vartheta$$

TABLE 1.

Inflow velocities.

Ship speed ahead	7.0 knots
Ship speed astern	3.5 knots
Effective wake fraction	w =0.25

Radial wake distribution

radius x	$\frac{1-w_x}{1-w}$
0.95	1.274
0.90	1.218
0.80	1.066
0.70	0.933
0.60	0.839
0.50	0.785
0.40	0.752
0.30	0.680

TABLE 2.

Dimensionless constans.

KQ = shaft torque/$\rho\ n^2.D^5$

KT = thrust/$\rho\ n^2.D^4$

CRH=hydrodynamic blade spindle torque/$\rho\ n^2.D^5$

CRHI=frictionless blade spindle torque/$\rho\ n^2.D^5$

Skew $_{.8R}$=17.6%

	non ventilated				1 side ventilated				2 sides ventilated			
operating condition	10KQ	KT	100. CRH	100. CRHI	10KQ	KT	100. CRH	100. CRHI	10KQ	KT	100. CRH	100. CRHI
1 zero pitch.7R	0.052	0.027	-0.579	-0.594	0.017	0.016	-0.175	-0.197	0.013	0.016	-0.055	-0.077
2 bollard ahead	0.173	0.196	-0.228	-0.348	0.156	0.165	-0.230	-0.367	0.152	0.164	-0.228	-0.366
3 bollard astern	0.171	-0.095	-0.770	-0.448	0.071	-0.053	-0.112	-0.022	0.068	-0.051	-0.009	0.082
4 free running ahead	0.171	0.160	-0.192	-0.356	0.168	0.158	-0.192	-0.346	0.168	0.158	-0.192	-0.346
5 free running ahead	0.170	-0.086	-0.791	-0.465	0.094	-0.070	-0.089	0.011	0.093	-0.070	-0.024	0.076

TABLE 3.

Dimensionless constants.

KQ = shaft torque/$\rho\ n^2.D^5$ KT=thrust/ $\rho\ n^2.D^4$

CRH=hydrodynamic blade spindle torque/$\rho\ n^2.D^5$

CRHI=frictionless blade spindle torque/ $\rho\ n^2.D^5$

$Skew_{.8R}$=8.8%

	non ventilated				1 side ventilated			
operating condition	10KQ	KT	100. CRH	100. CRHI	10KQ	KT	100. CRH	100. CRHI
1 zero pitch .7R	0.046	0.023	-0.488	-0.519	0.017	0.014	-0.154	-0.174
2 bollard ahead	0.175	0.198	-0.046	-0.111	0.155	0.167	-0.046	-0.160
3 bollard astern	0.170	-0.106	-0.773	-0.515	0.074	-0.057	-0.165	-0.095
4 free running ahead	0.171	0.160	-0.032	-0.165	0.168	0.158	-0.032	-0.159
5 free running astern	0.169	-0.096	-0.793	-0.520	0.099	-0.075	-0.163	-0.086

LIPS N.V. - DRUNEN - NEDERLAND

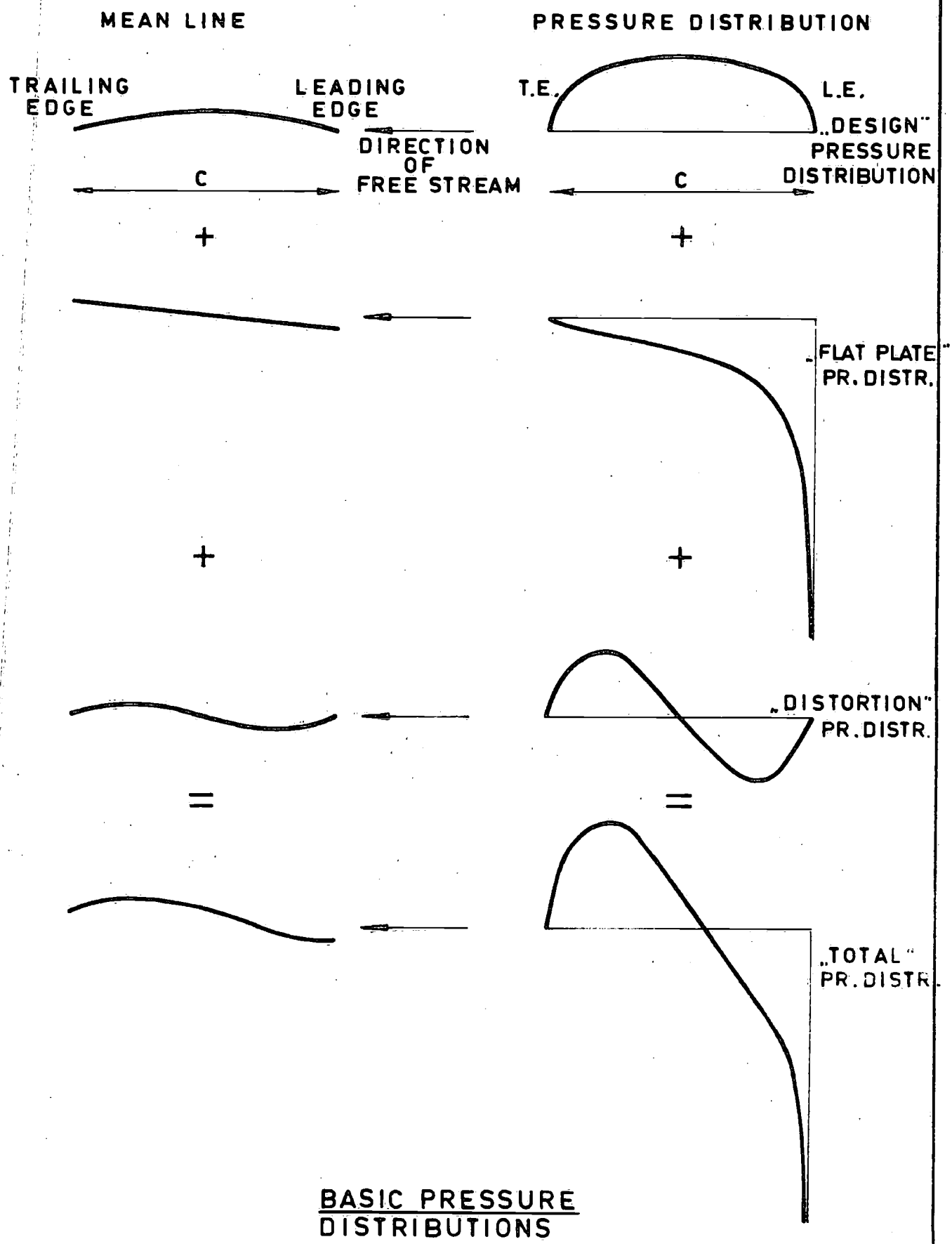

BASIC PRESSURE DISTRIBUTIONS

FIGURE 1

000.D9

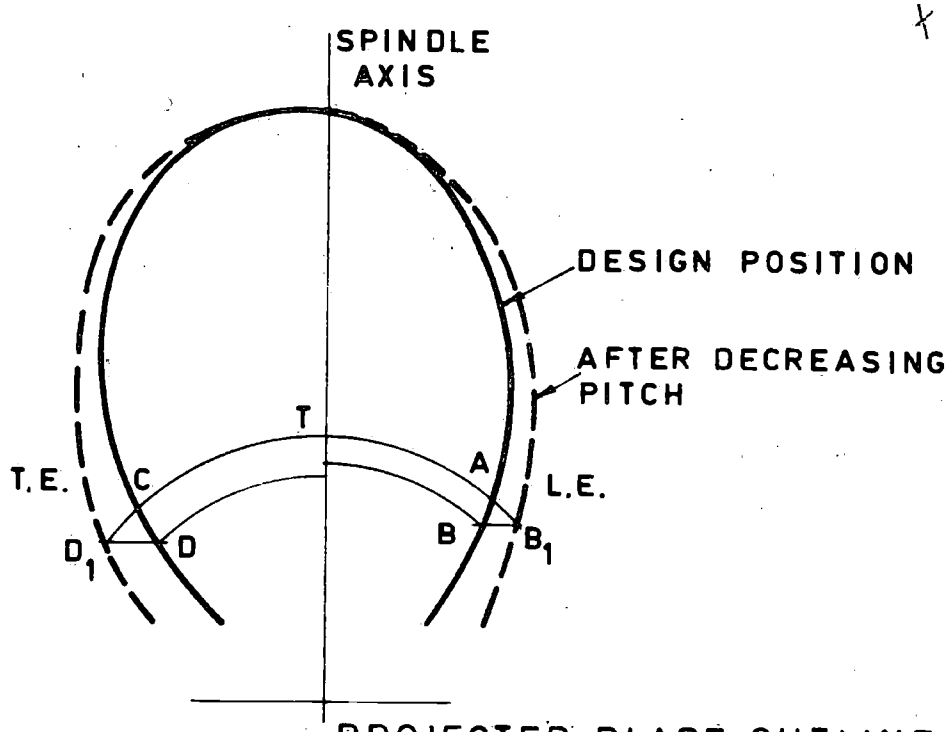

PROJECTED BLADE OUTLINE
AT DIFFERENT PITCH SETTINGS

FIGURE 2

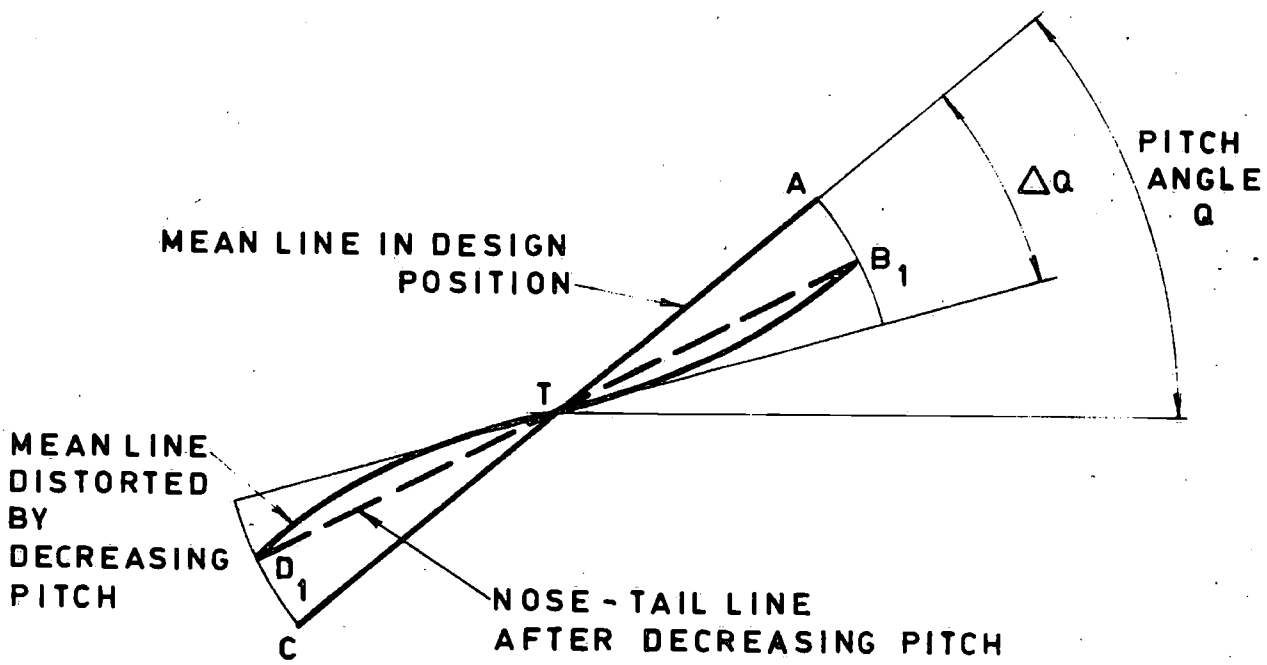

MEAN LINE DISTORTION

FIGURE 3

CHARACTERISTIC OPERATING CONDITIONS

1 ZERO THRUST POINT
2 BOLLARD AHEAD
3 BOLLARD ASTERN
4 FREE RUNNING AHEAD
5 FREE RUNNING ASTERN

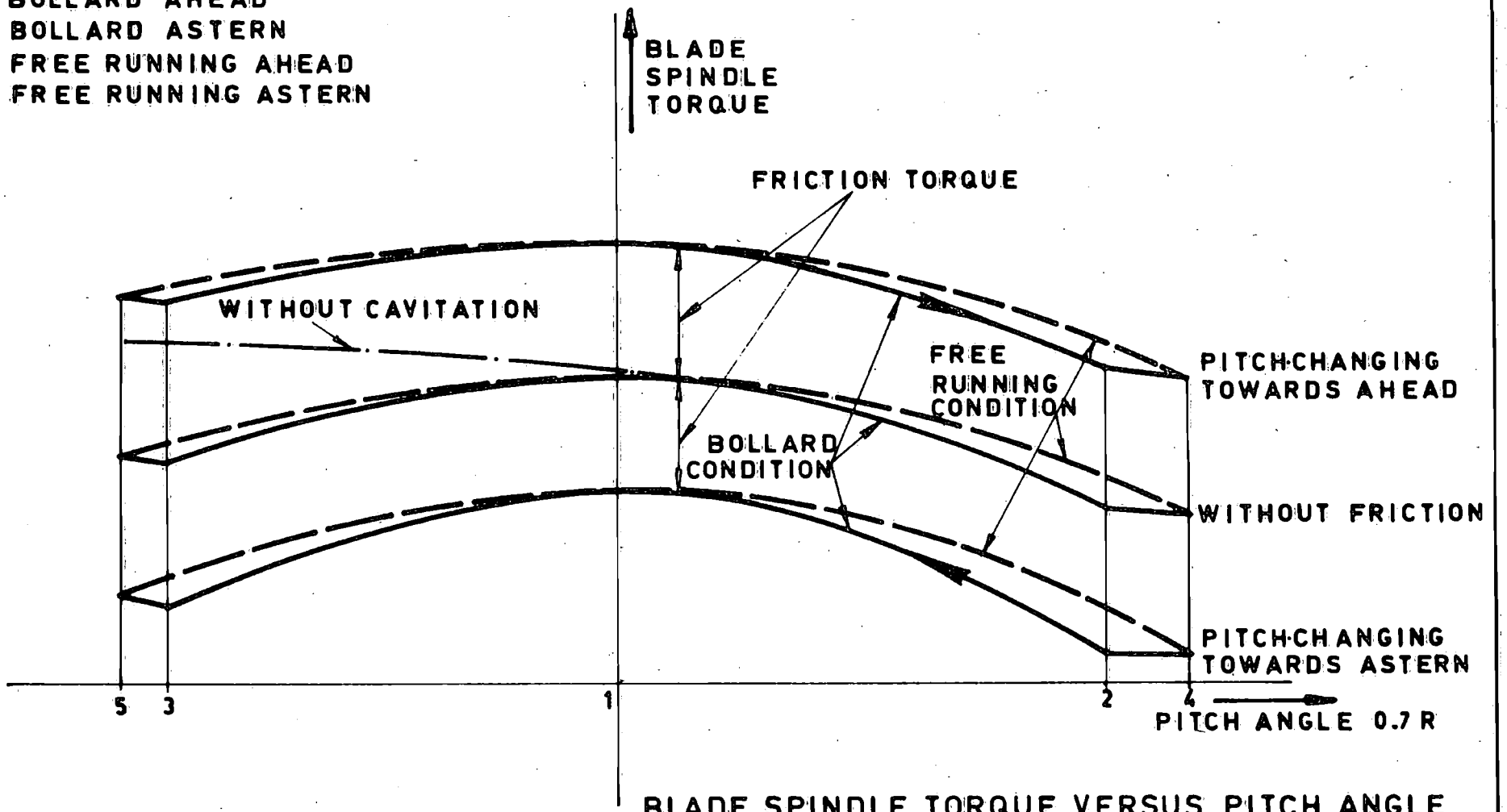

BLADE SPINDLE TORQUE VERSUS PITCH ANGLE AT MAXIMUM ROTATIONAL SPEED

FIGURE 4

LIPS N.V. - DRUNEN - NEDERLAND

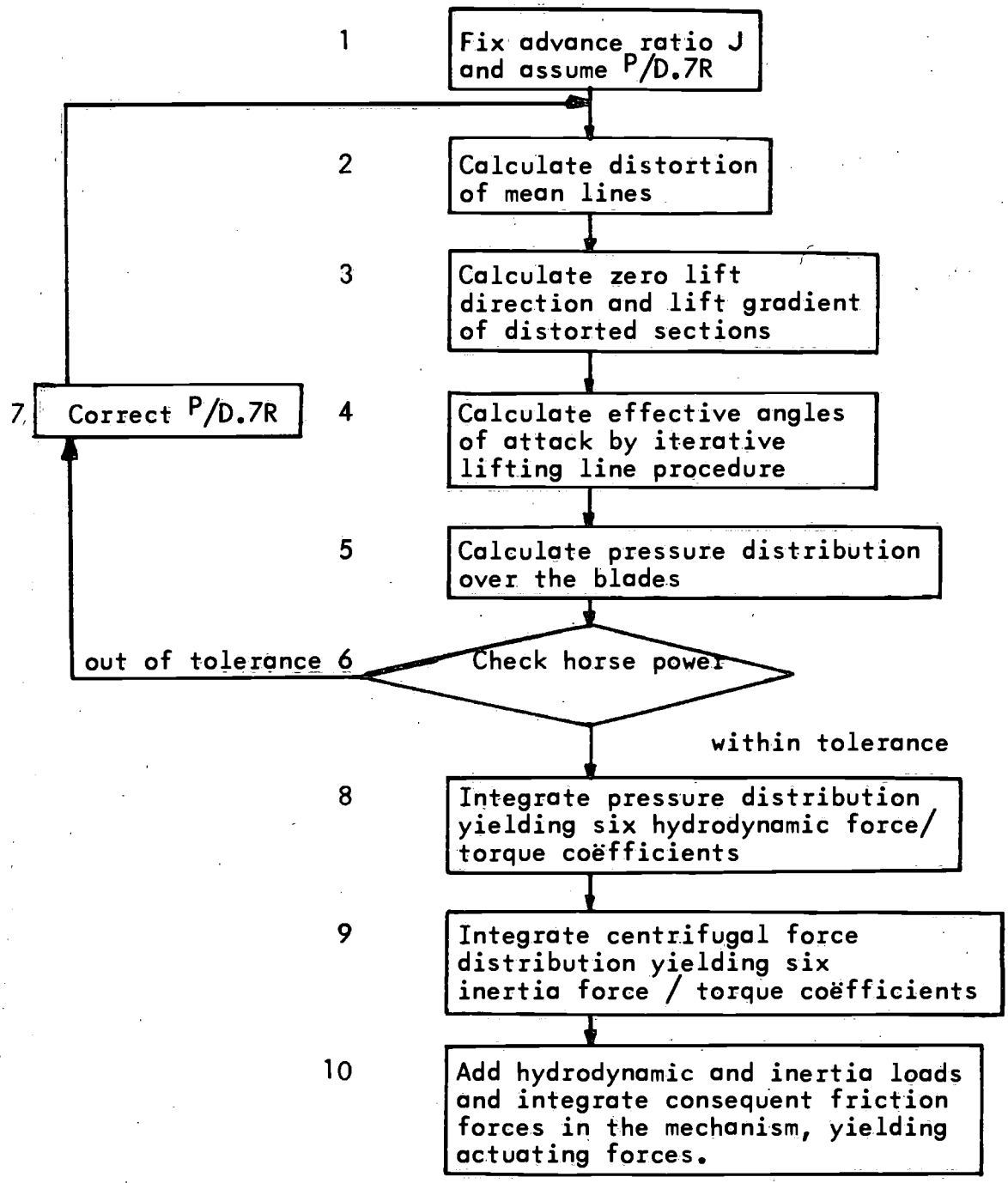

Flow chart of the calculation of actuating forces.

Figure 5

THICKNESS	CAMBER	PITCH	RADIUS
8.5		1400	1.0
21	7.5	1400	0.95
25.5	9.6	1400	0.9
35	14.6	1400	0.8
44	19.0	1400	0.7
53.5	22.1	1400	0.6
65	16.3	1358	0.5
80	7.2	1239	0.4
104	0.8	1050	0.3
64			

SPINDLE AXIS

EXPANDED BLADE OUTLINE

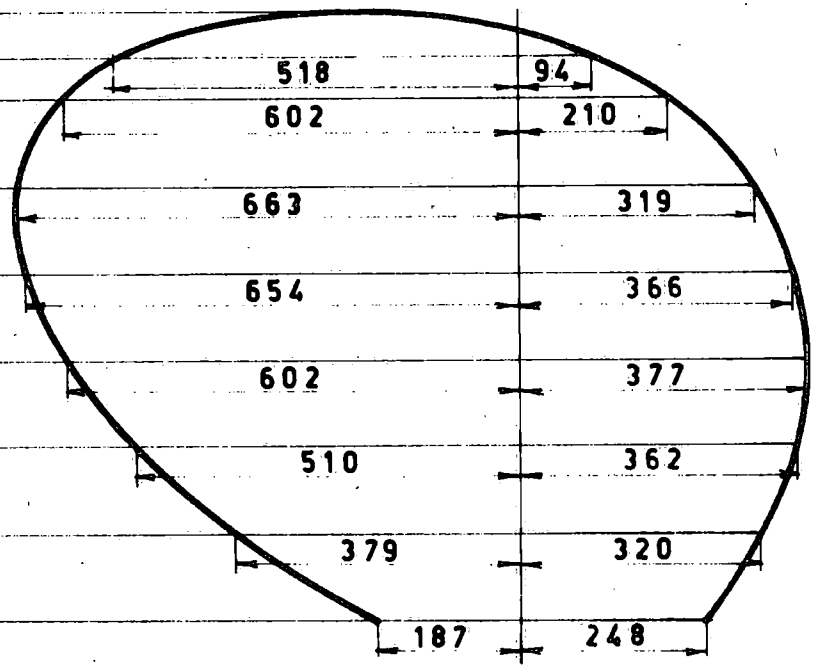

DIAMETER 2300 mm
NUMBER OF BLADES 3
EXPANDED BLADE AREA RATIO 0.528
ENGINE OUTPUT 1250 B.H.P. x 300 R.P.M.

NACA a = 0.8 MEAN LINE
NACA 16 THICKNESS FORM

PROPELLER DIMENSIONS

FIGURE 6

LIPS N.V. - DRUNEN - NEDERLAND

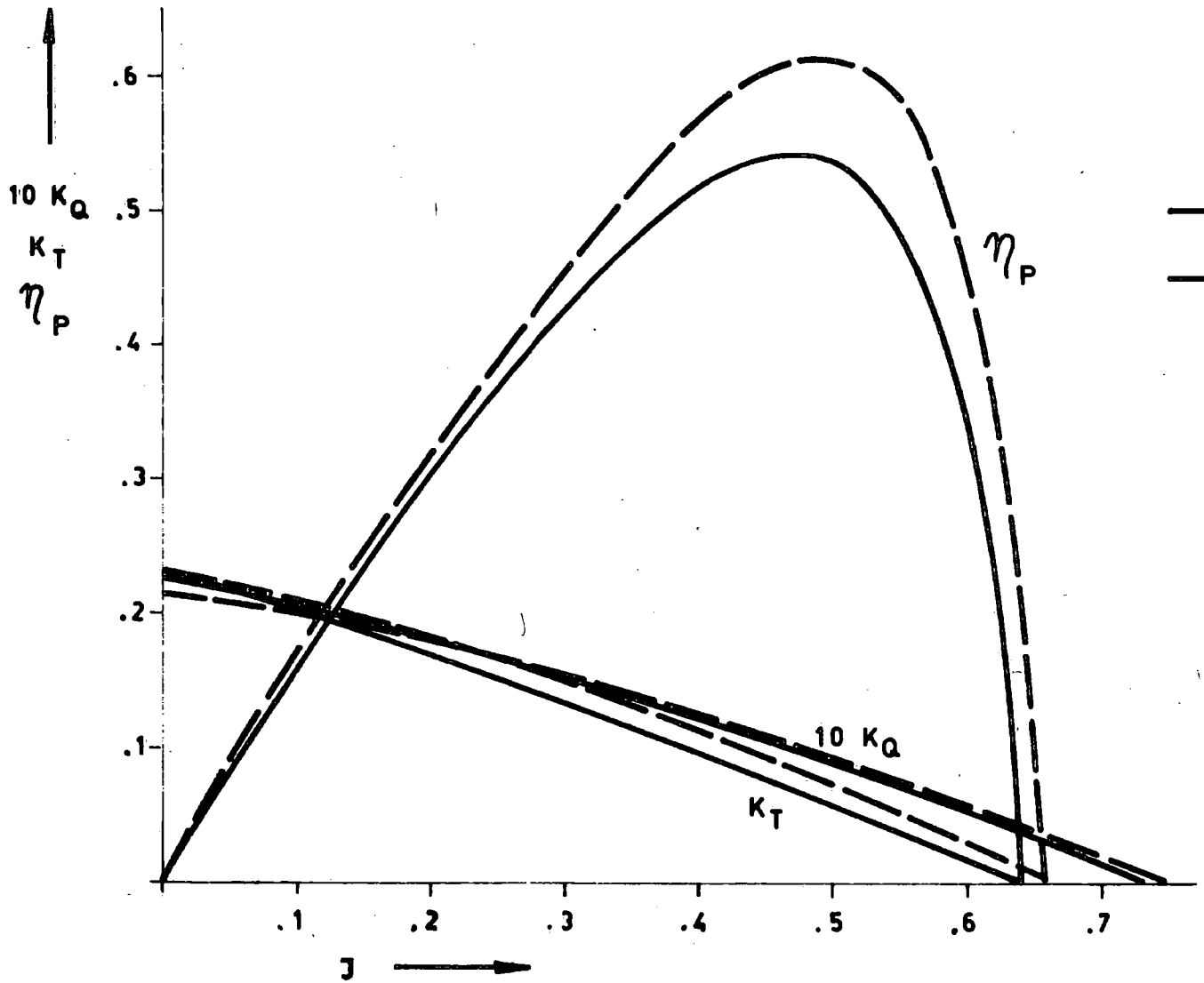

PROPELLER OF FIGURE 6 (CALCULATED)

PROPELLER B 3-50 (MEASURED)

P/D = 0.6

OPEN WATER DIAGRAM

FIGURE 7

LIPS N.V. - DRUNEN - NEDERLAND

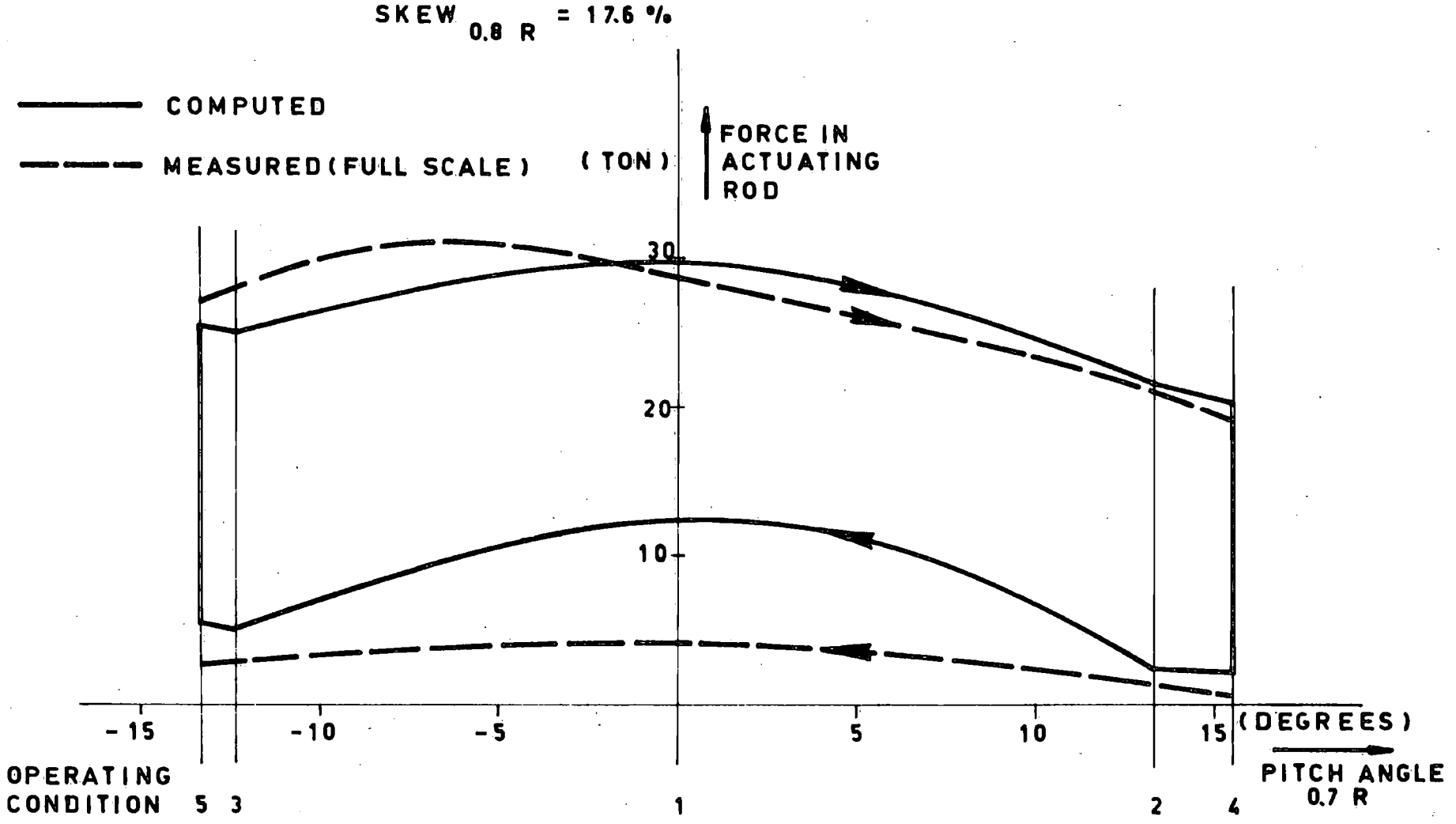

COMPUTED AND MEASURED ACTUATING FORCES

FIGURE 8

LIPS N.V. - DRUNEN - NEDERLAND

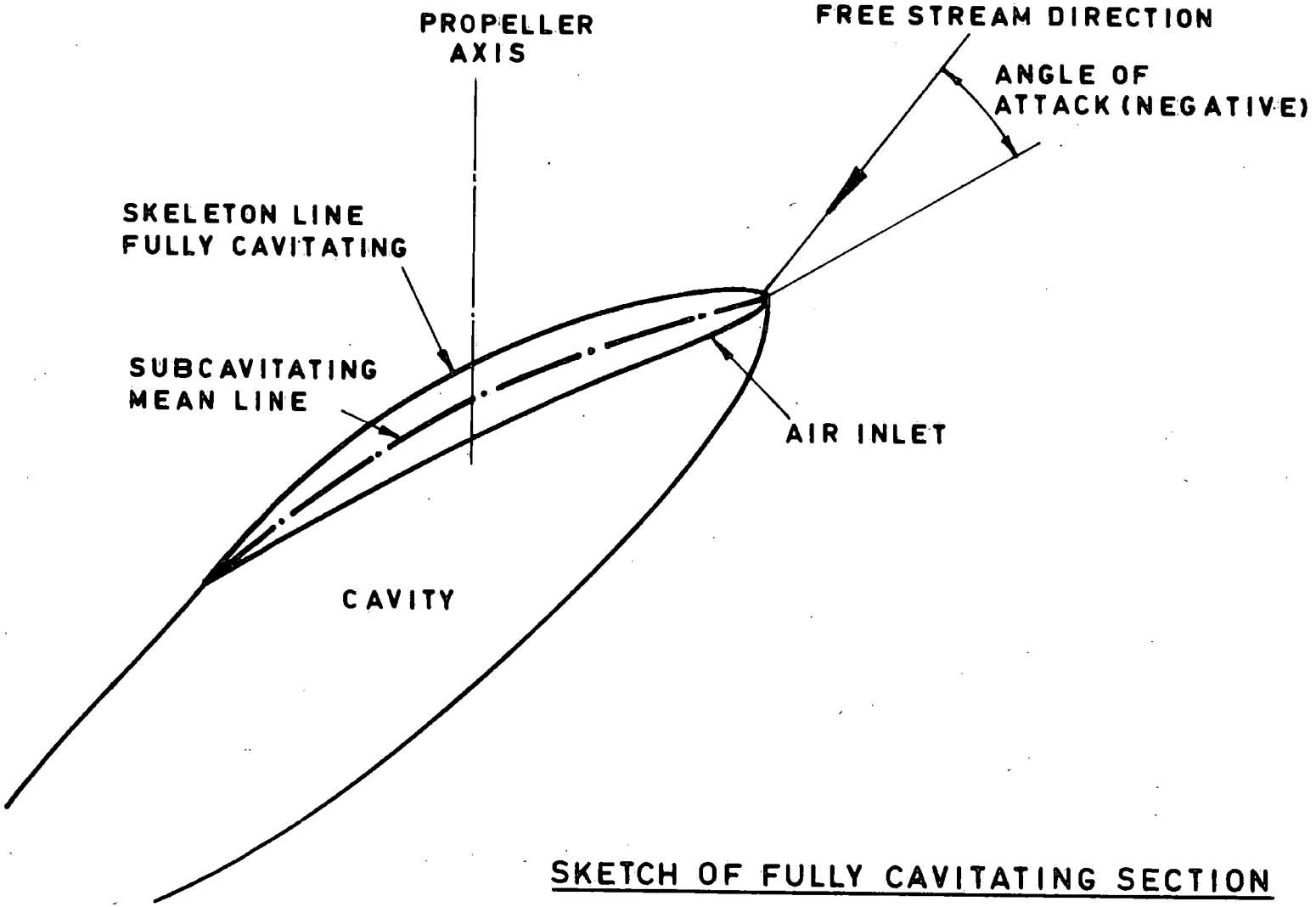

SKETCH OF FULLY CAVITATING SECTION

FIGURE 9

LIPS N.V. - DRUNEN - NEDERLAND

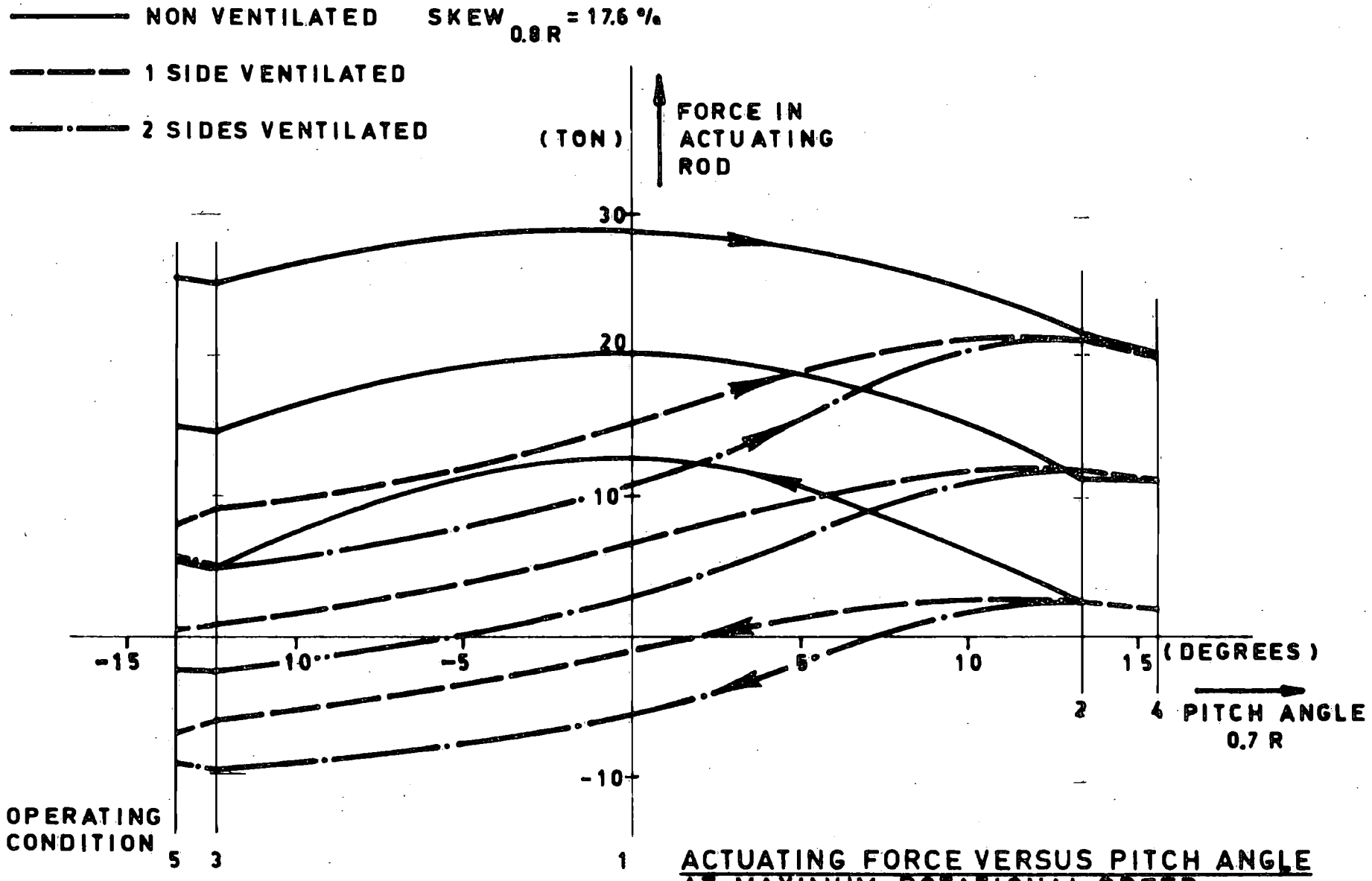

ACTUATING FORCE VERSUS PITCH ANGLE AT MAXIMUM ROTATIONAL SPEED

FIGURE 10

LIPS N.V. - DRUNEN - NEDERLAND

LIPS N.V. - DRUNEN - NEDERLAND

OPERATING CONDITION 1 (ZERO THRUST)

$SKEW_{0.8\,R}$ = 17.6 %

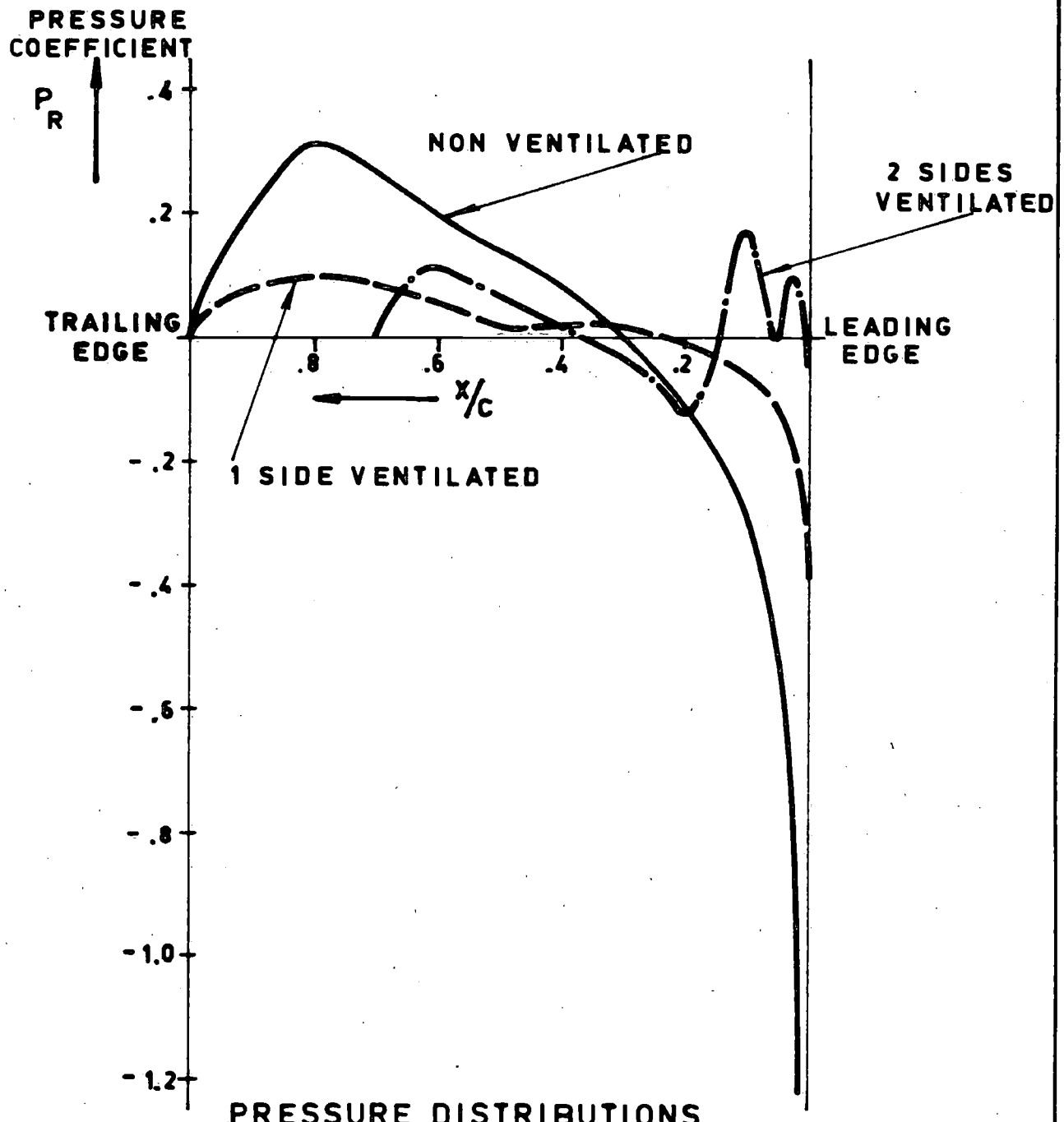

PRESSURE DISTRIBUTIONS AT 0.7 RADIUS

FIGURE 11

030-D9

OPERATING CONDITIONS 2 AND 4
(BOLLARD AHEAD AND
FREE RUNNING AHEAD)
$SKEW_{0.8\,R}$ = 17.6 %

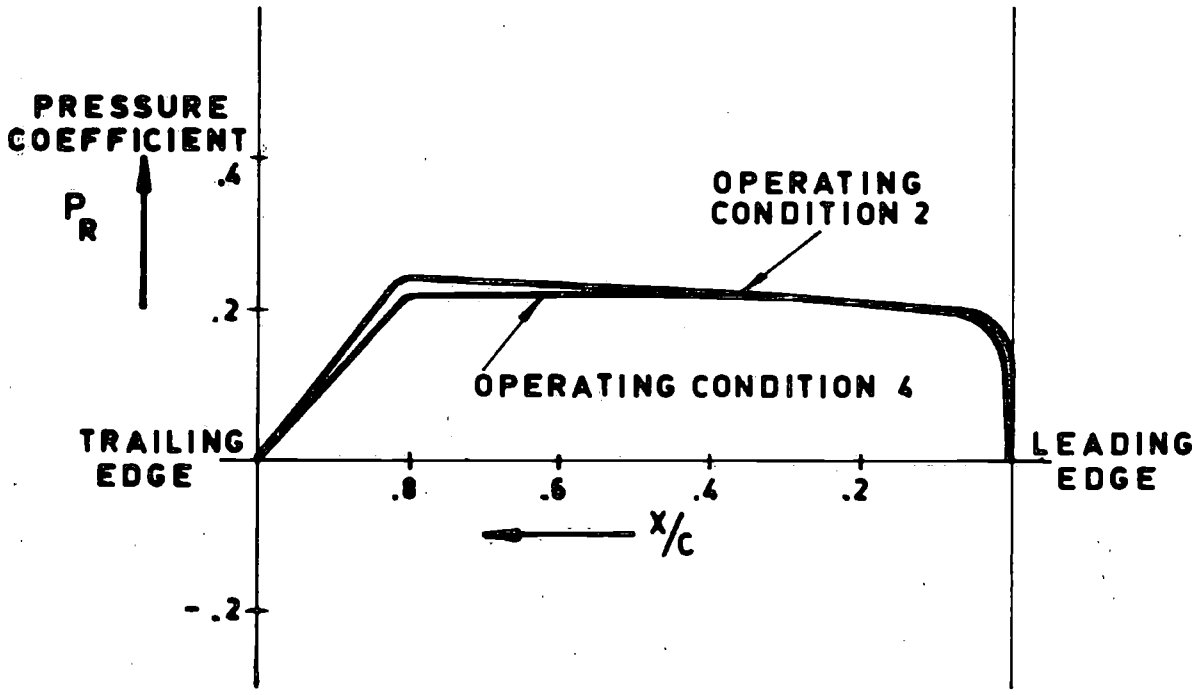

PRESSURE DISTRIBUTIONS
AT 0.7 RADIUS.(IDENTICAL IN
NON VENTILATED AND IN
VENTILATED CONDITION)

FIGURE 12

LIPS N.V. - DRUNEN - NEDERLAND

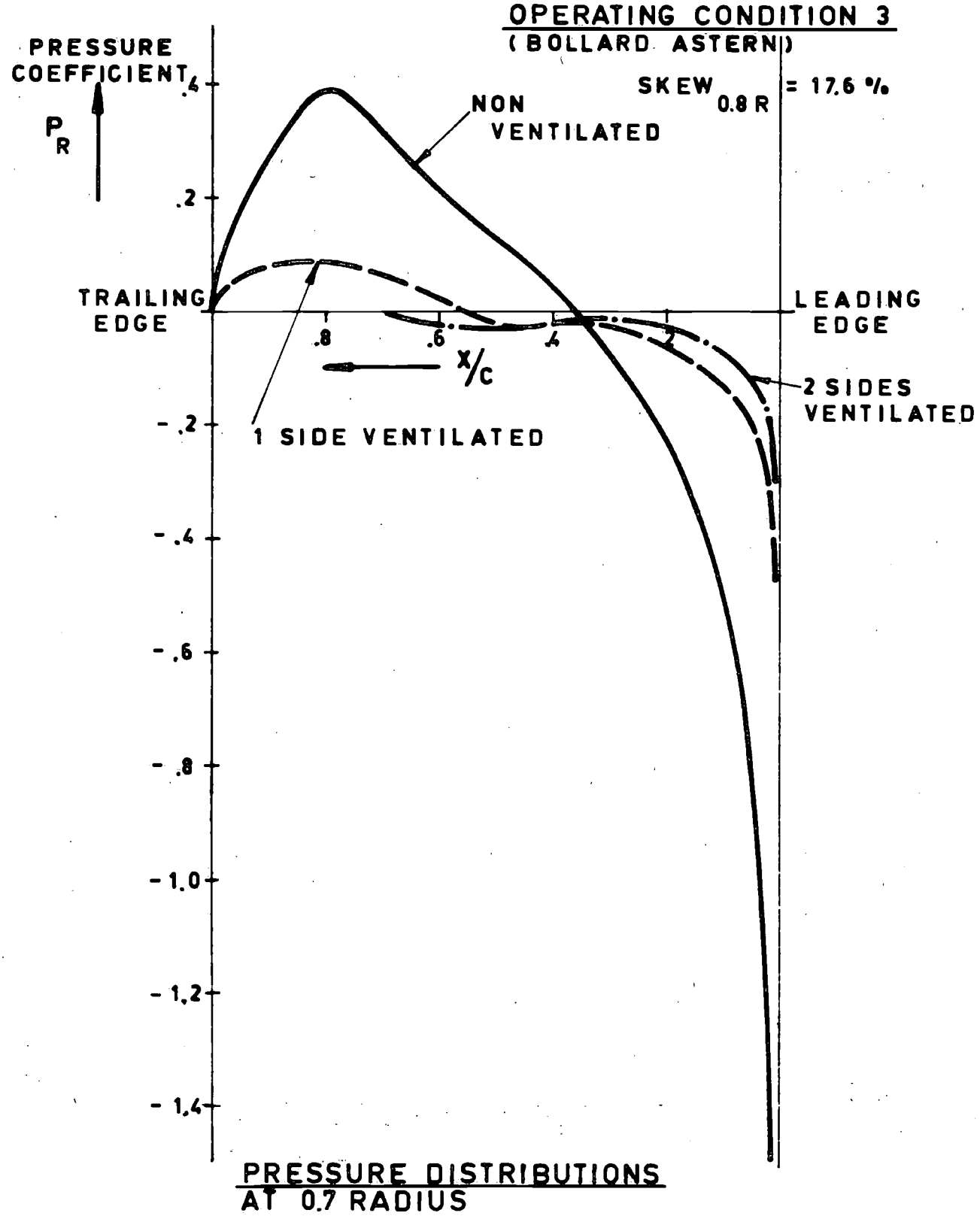

PRESSURE DISTRIBUTIONS
AT 0.7 RADIUS

FIGURE 13

LIPS N.V. - DRUNEN - NEDERLAND

OPERATING CONDITION 5.
(FREE RUNNING ASTERN)

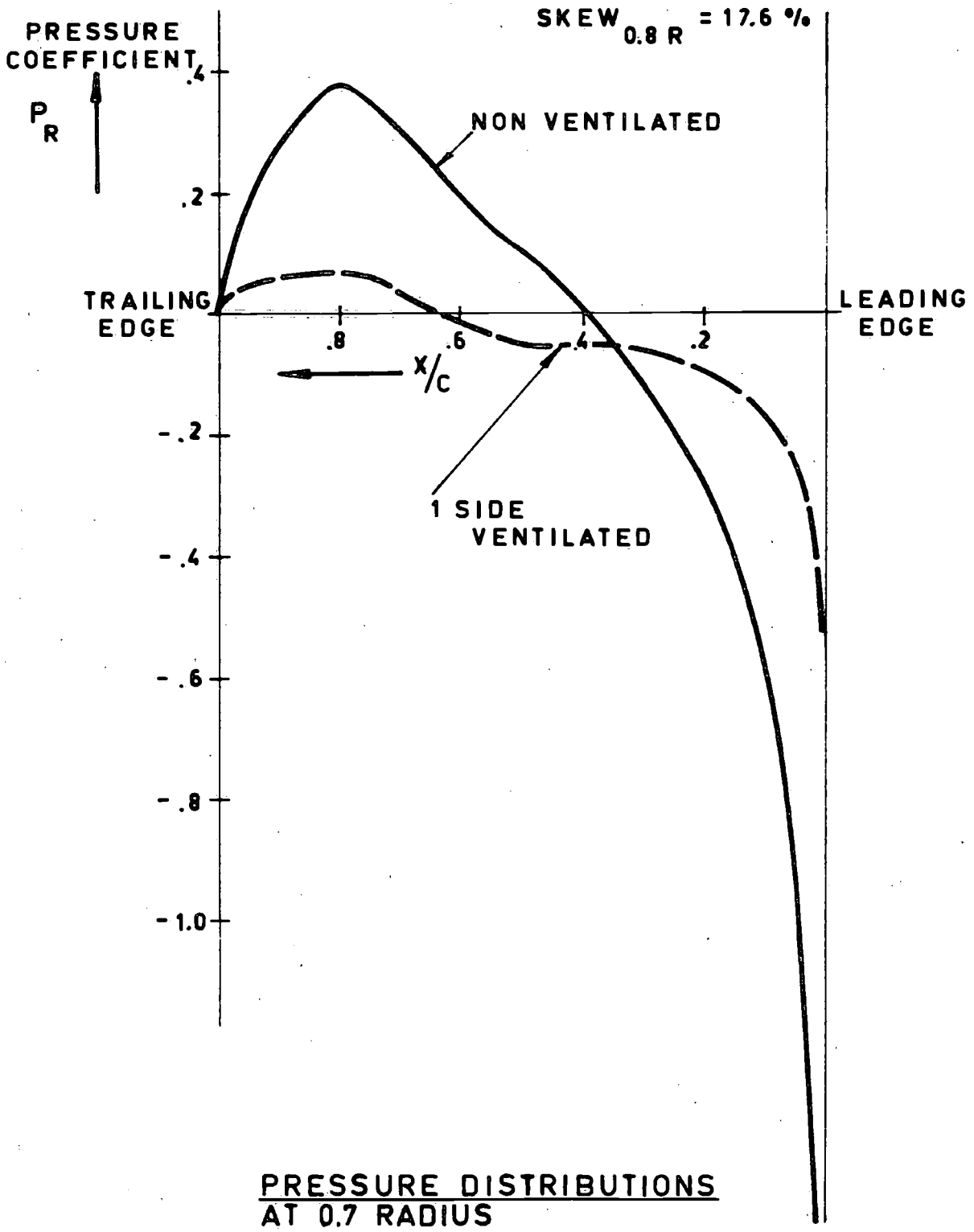

PRESSURE DISTRIBUTIONS
AT 0.7 RADIUS

FIGURE 14

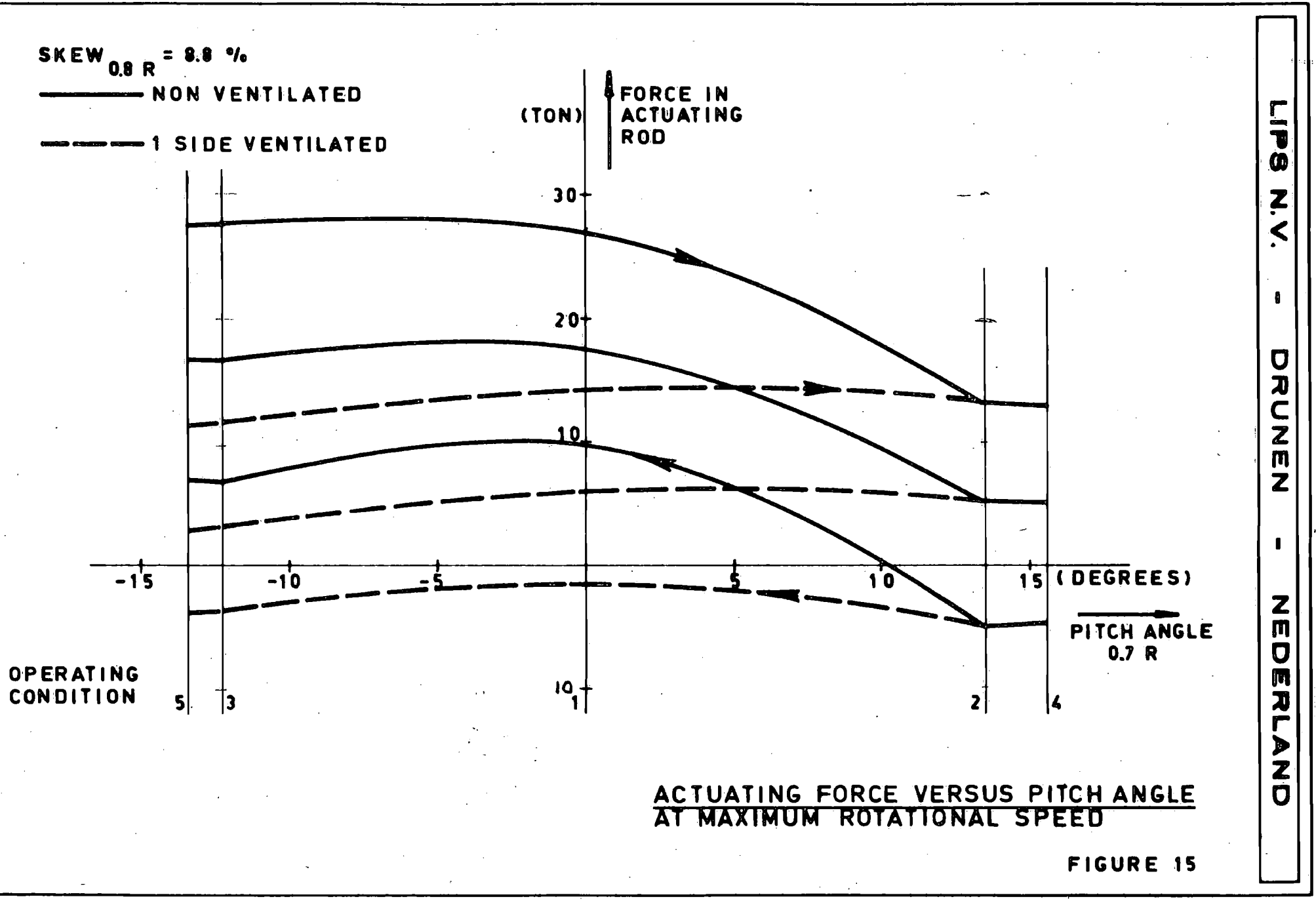

ACTUATING FORCE VERSUS PITCH ANGLE AT MAXIMUM ROTATIONAL SPEED

FIGURE 15

LIPS N.V. - DRUNEN - NEDERLAND

OPERATING CONDITION 1 (ZERO THRUST)

$SKEW_{0.8\,R}$ = 8.8 %

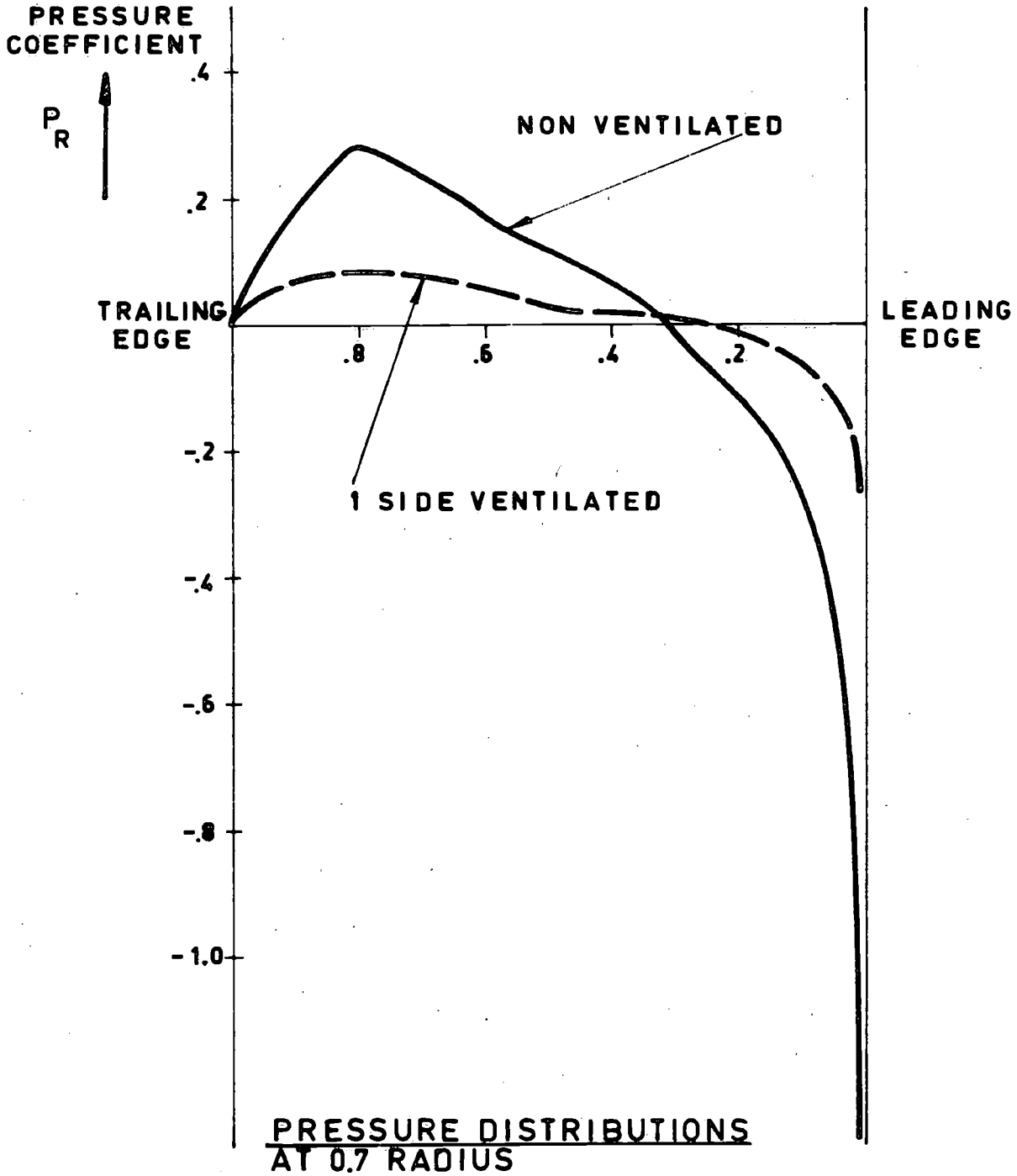

PRESSURE DISTRIBUTIONS AT 0.7 RADIUS

FIGURE 16

LIPS N.V. - DRUNEN - NEDERLAND

OPERATING CONDITIONS 2 AND 4
(BOLLARD AHEAD AND FREE RUNNING AHEAD)

SKEW $_{0.8\,R}$ = 8.8 %

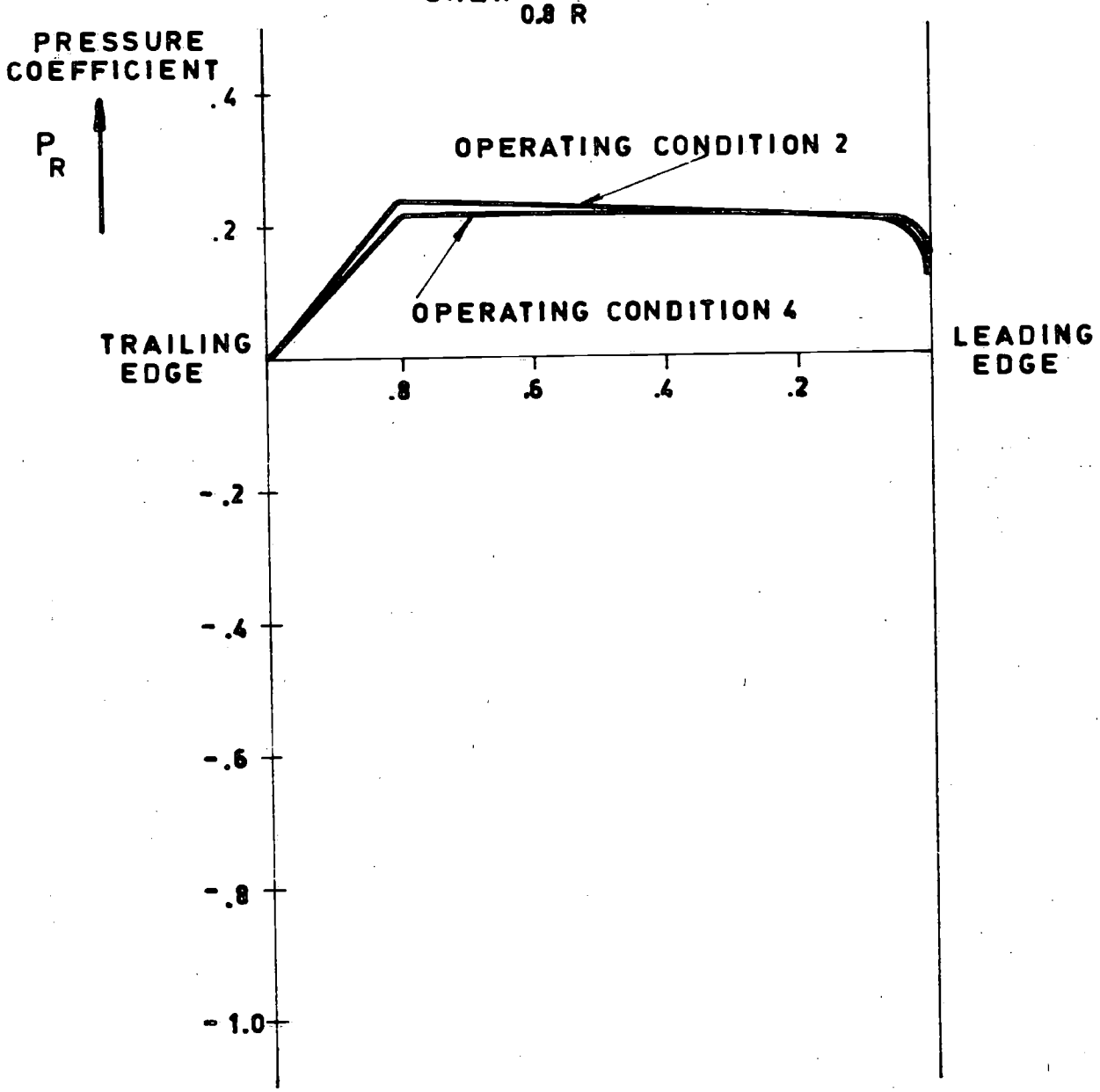

PRESSURE DISTRIBUTIONS AT 0,7 RADIUS (IDENTICAL IN NON VENTILATED AND IN VENTILATED CONDITION)

FIGURE 17

000-D9

OPERATING CONDITION 3
(BOLLARD ASTERN)

$SKEW_{0.8\,R}$ = 8.8 %

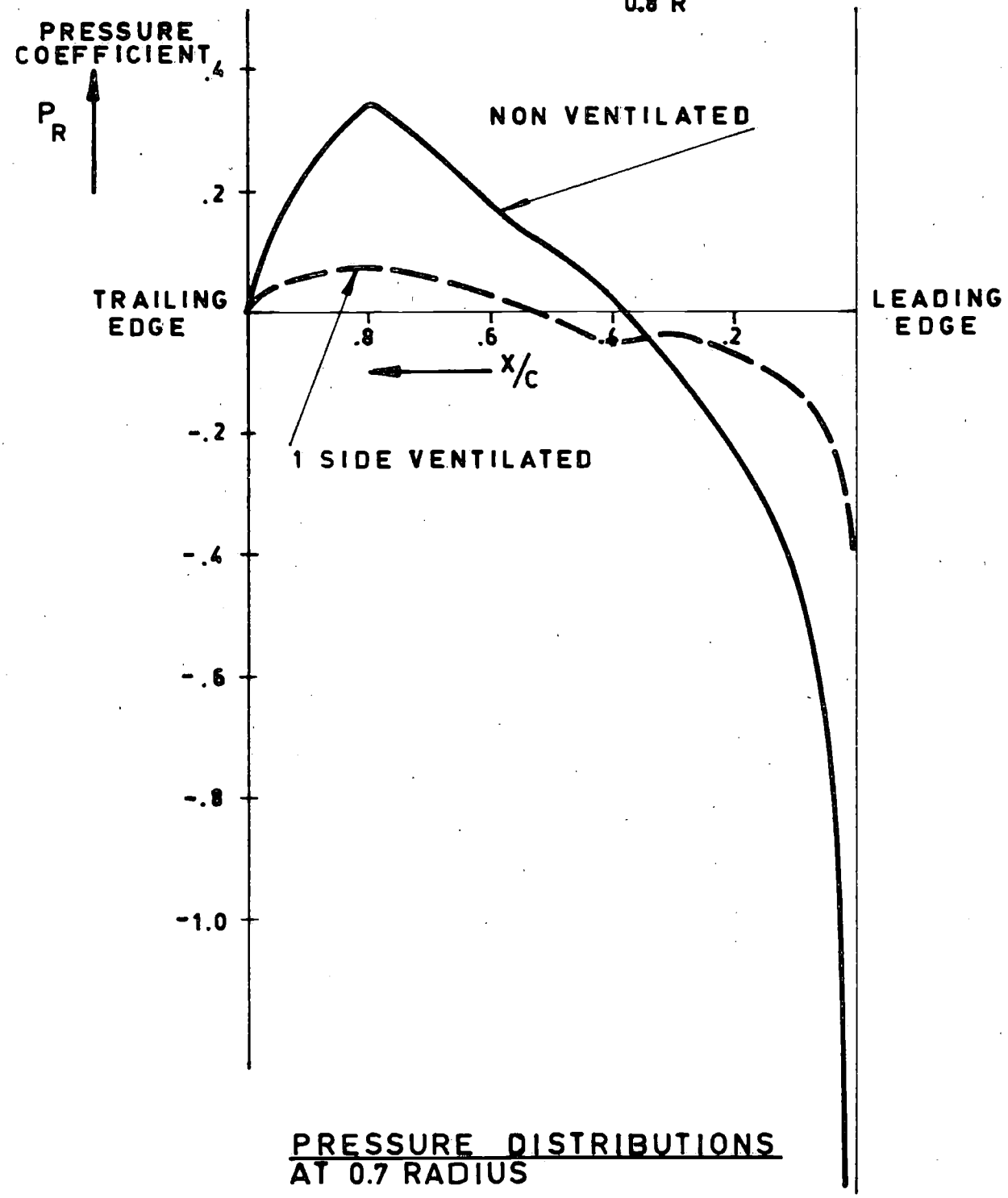

PRESSURE DISTRIBUTIONS
AT 0.7 RADIUS

FIGURE 18

LIPS N.V. - DRUNEN - NEDERLAND

OPERATING CONDITION 5
(FREE RUNNING ASTERN)

$SKEW_{0.8\,R} = 8.8\ \%$

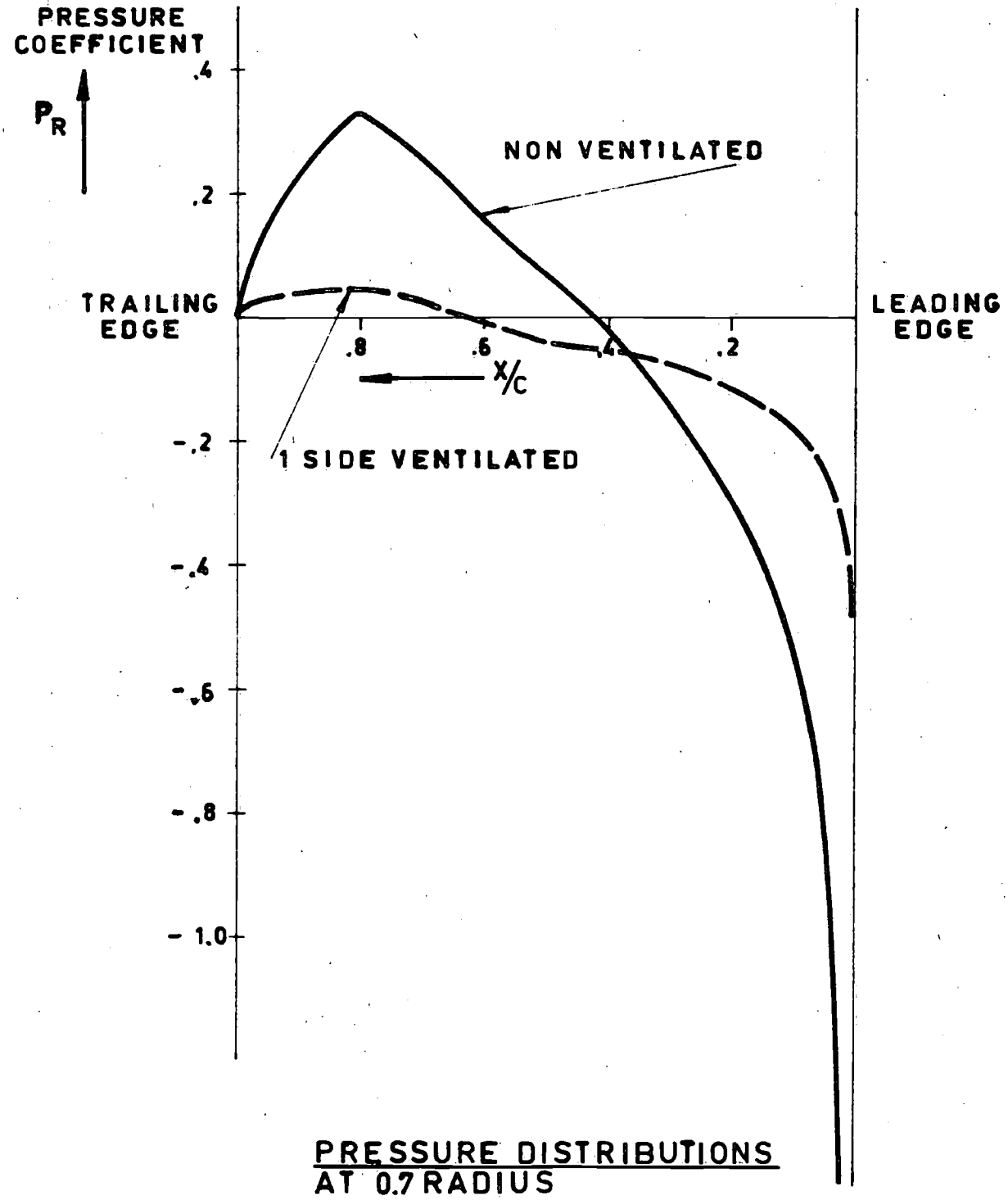

PRESSURE DISTRIBUTIONS
AT 0.7 RADIUS

FIGURE 19